

WonderTurbo: Generating Interactive 3D World in 0.72 Seconds

Chaojun Ni^{*1,2} Xiaofeng Wang^{*1,3} Zheng Zhu^{*1✉} Weijie Wang^{*1,4} Haoyun Li^{1,3}
 Guosheng Zhao^{1,3} Jie Li¹ Wenkang Qin¹ Guan Huang¹ Wenjun Mei^{2✉}
¹GigaAI ²Peking University
³Institute of Automation, Chinese Academy of Sciences ⁴Zhejiang University

Project Page: <https://wonderturbo.github.io>

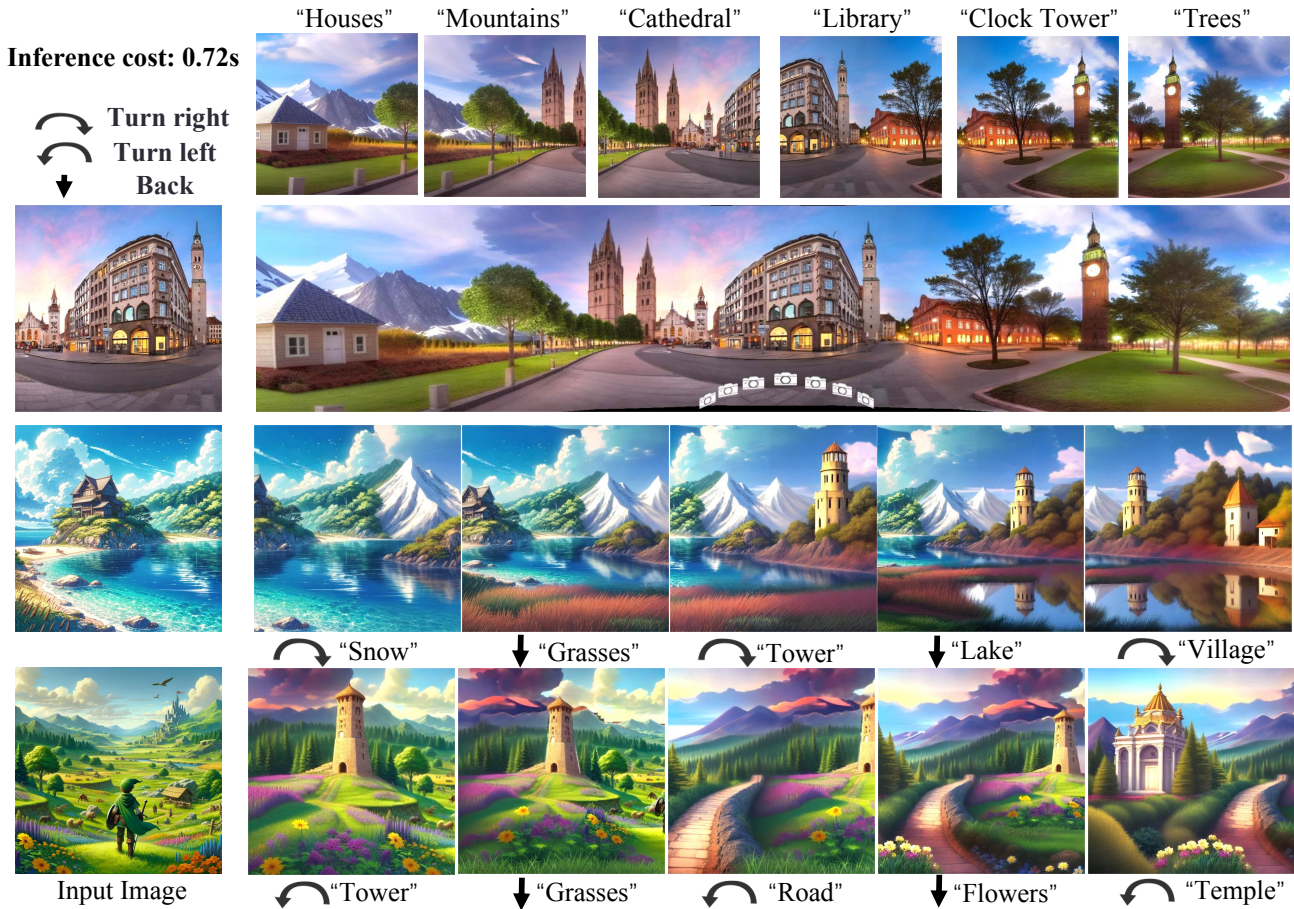


Figure 1. Beginning with a single image, users can freely adjust the viewpoint and interactively control the generation of a 3D scene, each interaction requiring only 0.72 seconds.

Abstract

Interactive 3D generation is gaining momentum and capturing extensive attention for its potential to create immersive virtual experiences. However, a critical challenge in current 3D generation technologies lies in achieving real-time

interactivity. To address this issue, we introduce WonderTurbo, the first real-time interactive 3D scene generation framework capable of generating novel perspectives of 3D scenes within 0.72 seconds. Specifically, WonderTurbo accelerates both geometric and appearance modeling in 3D scene generation. In terms of geometry, we propose StepSplat, an innovative method that constructs efficient 3D geometric representations through dynamic updates, each

^{*}These authors contributed equally to this work. [✉]Corresponding authors: Zheng Zhu, zhengzhu@ieec.org, Wenjun Mei, mei@pku.edu.cn.

taking only 0.26 seconds. Additionally, we design *QuickDepth*, a lightweight depth completion module that provides consistent depth input for *StepSplat*, further enhancing geometric accuracy. For appearance modeling, we develop *FastPaint*, a 2-steps diffusion model tailored for instant inpainting, which focuses on maintaining spatial appearance consistency. Experimental results demonstrate that *WonderTurbo* achieves a remarkable $15\times$ speedup compared to baseline methods, while preserving excellent spatial consistency and delivering high-quality output.

1. Introduction

The online generation of 3D from a single image [64, 65], which involves instant creation and updating of 3D scenes, has attracted significant attention. Compared with offline generation methods [10, 21, 30, 32, 34, 66], which generate a fixed 3D scene based on user texts and input images, online generation allows users to interactively create and edit 3D content, enhancing creation efficiency and flexibility.

Despite these advantages, existing online 3D scene generation methods [64, 65] still face significant challenges, primarily due to the low inference efficiency. This efficiency bottleneck largely stems from the time-consuming processes of optimizing geometric details and generating or refining new view appearances. Specifically, 3D scene representation methods like 3D Gaussian Splattings (3DGS) [23] require iterative training to update new geometries, while appearance refinement is based on diffusion-based image inpainting models [37] that require extensive inference steps, further increasing computational overhead. For example, the current fastest online 3D generation approach, *WonderWorld* [64], takes nearly 10 seconds to update a single 3D view, which falls short of real-time performance expectations. Although some works [33, 40, 45–47, 72, 72] on generating novel views from a single image improve in speed, these methods only support generating views within small viewpoint changes.

In this paper, we present *WonderTurbo*, a novel framework designed for real-time interactive 3D scene generation. To address the critical challenges of inference efficiency, we optimize both geometric representation and appearance modeling. For geometric optimization, we introduce *StepSplat*, a scalable method that accelerates 3D scene expansion in 0.26 seconds. Unlike conventional 3DGS methods [23, 32, 55, 60, 69] that rely on iterative training to update 3D representations, *StepSplat* leverages insights from recent feed-forward approaches [7, 8, 52, 54] to perform direct inference 3DGS. Moreover, *StepSplat* extends the feed-forward paradigm to interactive 3D geometric representation, ensuring consistency across dynamic viewpoint changes. This is achieved through the maintenance of a feature memory module, which adaptively constructs cost vol-

umes as the viewpoint changes. Meanwhile, to further enhance depth coherence, we incorporate a lightweight depth completion module, *QuickDepth*, to provide a consistent depth prior for *StepSplat* to construct the cost volume. On the appearance front, we propose *FastPaint*, a highly efficient method for real-time appearance refinement. In contrast to traditional diffusion-based inpainting methods [37], which require dozens of inference steps to refine appearance modeling, *FastPaint* achieves comparable results with only 2 inference steps while preserving spatial appearance consistency.

We present the results of various camera setups, including a panoramic camera path and two casual walking camera paths as shown in Fig. 1. The results demonstrate that *WonderTurbo* can accurately generate 3D scenes based on user-provided text while maintaining high consistency. Furthermore, our model achieves leading performance in CLIP-based metrics [35, 49] and user study win rates, while significantly boosting speed, achieving a $15\times$ acceleration.

The main contributions of this paper are summarized as follows:

- We present *WonderTurbo*, the first real-time (inference cost: 0.72 seconds) 3D scene generation method that allows users to interactively create diverse and cohesively connected scenes.
- For geometric efficiency optimization, the proposed *StepSplat* extends feed-forward paradigm to interactive 3D geometric representation, accelerating the expansion of 3D scenes within 0.26 seconds. Besides, *QuickDepth* is introduced to ensure depth consistency during viewpoint changes. For appearance modeling efficiency, we present *FastPaint* for image inpainting with only 2-steps inference.
- We perform comprehensive experiments to validate that *WonderTurbo*, while achieving a $15\times$ acceleration, surpasses other methods in generating high-quality 3D scenes, both in geometry and appearance.

2. Related Work

2.1. Offline 3D Scene Generation from Single Image

Offline 3D scene generation from a single image [2, 10, 15, 21, 25, 30, 34, 59, 66] has been explored by various methods, which generally involve generating multiple views or panoramas of a scene and subsequently transforming them into a 3D representation. Approaches such as *Text2Room* [21] and *LucidDreamer* [10] begin with a single input image and a user’s textual description, generate multiple images of the scene, and then employ 3D optimization to refine the scene and create a more accurate and consistent 3D representation. Meanwhile, *Wonderland* [26] predicts 3DGS in a feed-forward manner by constructing 3D reconstruction models based on a video

diffusion model’s latent space. In contrast, methods such as GenEx [30], Pano2Room [34], and Dreamscene360 [71] synthesize coherent panoramas by leveraging pretrained text-to-panorama diffusion models [16, 62], which are then elevated to 3D, ultimately producing explorable 3D worlds. However, these methods typically operate offline, preventing user interaction during the generation process. Furthermore, once the scene is generated, modifying or adjusting the layout or content becomes challenging.

2.2. Online 3D Scene Generation from Single Image

Some researches have focused on the online interactive generation of 3D scenes, which only requires an image to generate a new 3D scene and specify its content. WonderJourney [65] employs an LLM [4, 5, 20, 57] to generate scene descriptions, a text-driven pipeline for coherent 3D scene generation, and a vision-language model (VLM) [1, 24] for result verification, while allowing users to adjust text and control the generation of new 3D scenes. However, this process takes several minutes, making it unsuitable for interactive use. WonderWorld [64] reduces reconstruction time using Fast LAYered Gaussian Surfels (FLAGS) and generates geometrically consistent scenes with guided diffusion-based depth estimation, but still requires about 10 seconds per scene. In contrast, *WonderTurbo* achieves the generation of diverse scenes within 0.72 seconds through accelerations both in geometric and appearance modeling, meeting the needs for real-time interaction.

2.3. 3D Scene Representations

3DGS [23] has attracted significant attention, for its high efficiency and photorealistic rendering. However, a major limitation of traditional 3DGS-based methods [32, 50, 56, 60] is the need for per-scene optimization, which can be time-consuming. 2D Gaussian Splatting [22] addresses this by projecting 3DGS onto a 2D plane, allowing faster rendering while maintaining geometric accuracy. Additionally, WonderWorld [64] introduces FLAGS, which employs a multi-layered representation and geometry-based initialization to reduce the need for per-scene optimization.

However, these methods still require significant computational time. Therefore, recent work [7–9, 42, 52, 54, 61] has explored using feed-forward networks to predict 3D geometry from images. PixelSplat [7] predicts 3DGS distributions by learning from paired images and MVSplat [8] leverages multi-view correspondence information through the construction of a cost volume. These methods are not suitable for generating interactive 3D scenes, especially for scenarios with gradually increasing views. Moreover, their reliance on unsupervised depth estimation leads to poor generalization.

Recent explorations [51, 52, 54] have attempted to address these challenges. FreeSplat [52] reconstructs long

sequence inputs by constructing an adaptive cost volume between adjacent views and aggregating features through multi-scale structures. However, it lacks depth supervision and does not address the requirement for handling a gradually increasing number of views. DepthSplat [54] integrates monocular depth estimation priors [58] into the feed-forward process, but its generalization capability remains limited, and it does not meet the needs of gradually increasing views.

3. Method

3.1. Overall Framework of WonderTurbo

Interactive 3D scene generation [64, 65] is constrained by computational efficiency due to the time-consuming geometry and appearance modeling. WonderWorld [64] introduces FLAGS to accelerate geometric modeling. However, it still requires hundreds of iterations to optimize the geometry representation, and its appearance modeling relies on a pretrained diffusion model [37] that needs dozens of inference steps for inpainting. In contrast, *WonderTurbo* achieves real-time interactive 3D scene generation by accelerating both geometry and appearance modeling. Specifically, we propose *StepSplat* for geometric modeling acceleration, which directly infers 3DGS in 0.26 seconds. Within this framework, *QuickDepth* completes missing depth information in 0.24 seconds. For appearance modeling acceleration, we introduce *FastPaint*, which completes image inpainting in 0.22 seconds.

We present the pipeline of *WonderTurbo* in Fig. 2. At the i -th iteration, given a user-specified location, *FastPaint* leverages the rendered image I_{render}^i from the current 3D scene and a user-provided textual description to generate a new scene appearance I_{target}^i . Subsequently, *QuickDepth* generates depth maps D_{target}^i using the rendered depth map D_{render}^i and the newly generated appearance I_{target}^i , ensuring that the geometry of the newly generated scene aligns with the existing 3D scene. Finally, *StepSplat* takes the depth map D_{target}^i and the new scene appearance I_{target}^i as inputs, incrementally fusing G_{local}^i into the global representation G_{global}^i . In the following sections, we delve into the details of *StepSplat*, *QuickDepth* and *FastPaint*.

3.2. StepSplat

To accelerate the modeling of appearance, we introduce *StepSplat*. As shown in Fig. 3, *StepSplat* takes as input the pose P^i , image I_{target}^i , and corresponding depth D_{target}^i from *QuickDepth*, and first uses backbone to extract both the matching features F_m^i and image features F_e^i . Then, it queries the feature memory for nearby views’ matching features to construct cost volumes. Then, cost volumes is concatenated with F_e^i to predict Gaussian parameters. Meanwhile, we leverage consistent input depth from *QuickDepth*

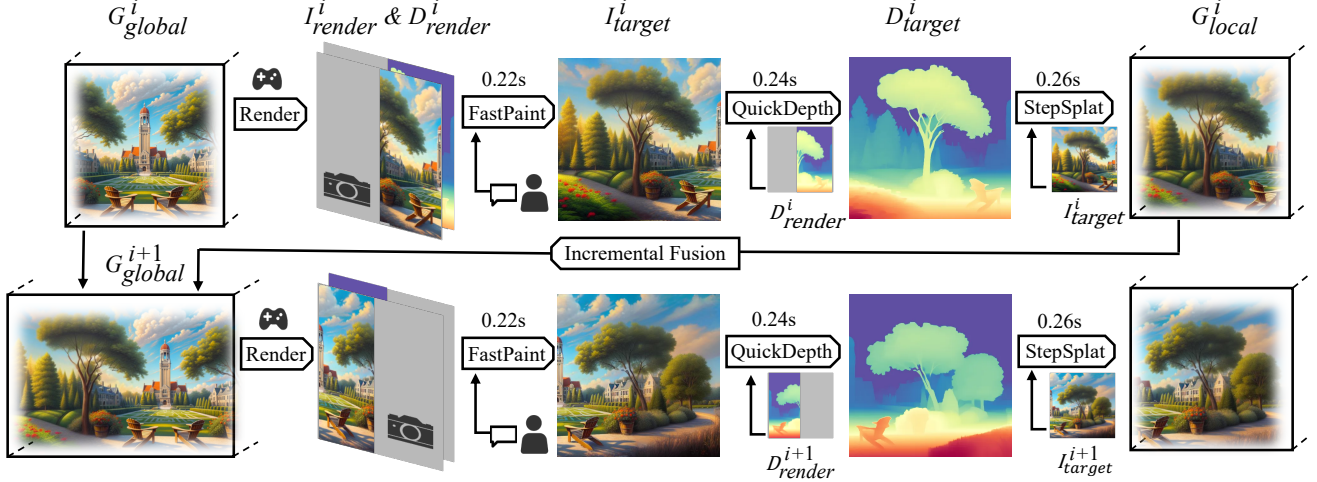


Figure 2. The pipeline of *WonderTurbo*. As the user moves the real-time rendering camera and inputs the text, the rendered image and depth map are then processed by *FastPaint* and *QuickDepth* to generate coherent geometry and appearance. Finally, *StepSplat* performs incremental fusion based on the outputs of *FastPaint* and *QuickDepth*.

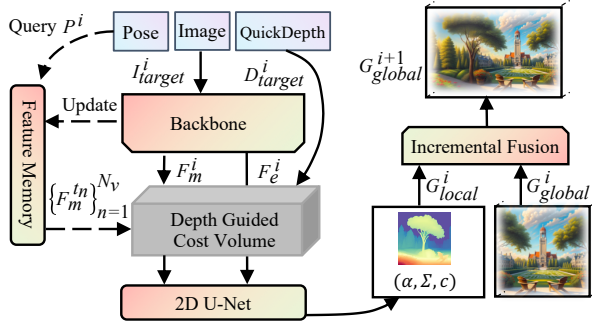


Figure 3. The structure of *StepSplat*.

as a geometric priority to construct the cost volume, which ensures the accuracy of Gaussian centers. Finally, an incremental fusion strategy merges newly generated G_{local}^i from the current view into the G_{global}^i , ensuring continuous and consistent 3D representation.

Feature Memory. We introduce the feature memory to store the matching features of previous views, which are used to build the late cost volume. Given the input images I_{target}^i and P^i , we first feed them into backbone to extract image features F_e^i and matching features F_m^i . Then, we construct a tuple (P^i, F_m^i) that is updated into the feature memory. To accelerate inference, we adapt RepVGG [13] as the backbone.

Depth Guided Cost Volume. For constructing the cost volume for the current view, we adaptively select N_v neighboring views from the feature memory and use the input depth from *QuickDepth* for the depth candidates of the cost volume. To achieve this, we first compute the distance between P^i and all stored poses $\{P^n\}_{n=1}^{i-1}$ in the Feature Memory:

$$d(P^n, P^i) = \|P^n - P^i\|_2, \quad (1)$$

where $\|\cdot\|_2$ represents the L2 norm. From these distances, we select the N_v closest poses to the current pose and extract their corresponding matching features from Memory as $\{(P^{t_n}, F_m^{t_n})\}_{n=1}^{N_v}$, where each t_n corresponds to one of the N_v closest poses.

For ensuring consistent 3D representation, inspired by Multi-View Stereo [17, 39, 51], we use D_{target}^i to guide the construction of the cost volume. Specifically, N_d depth candidates $\{d_s\}_{s=1}^{N_d}$ are uniformly sampled from R as:

$$R = \{d \mid (1-a) \cdot D_{target}^i \leq d \leq (1+a) \cdot D_{target}^i\}, \quad (2)$$

where a is the offset value used to adjust the depth candidate range. Then, each neighboring view’s matching feature $F_m^{t_n}$ is warped to the candidate depth d_s planes of the current view using the plane-sweep stereo algorithm [11], the feature warping is formulated as:

$$F_{d_s}^{t_n \rightarrow i} = \mathcal{W}(F_m^{t_n}, P^i, P^{t_n}, d_s), \quad (3)$$

where \mathcal{W} denotes the differentiable warping operation. We then compute the normalized dot-product correlation between the current view’s feature F_m^i and each warped neighboring feature $F_{d_s}^{t_n \rightarrow i}$, and average the correlation maps from all neighboring views:

$$S^i = \left[\frac{1}{N_v} \sum_{n=1}^{N_v} F_m^i \cdot F_{d_s}^{t_n \rightarrow i} \right]_{s=1}^{N_d}, \quad (4)$$

where N_d is the number of candidate depths, and the correlation maps from each depth are stacked to form the cost volume S^i . Meanwhile, an additional 2D U-Net [38] is used to further refine and upsample the cost volume. We normalize the cost volume S^i and perform a weighted average of all depth candidates to obtain the predicted depth map \hat{d} :

$$\hat{d} = \text{softmax}(S^i) \cdot d. \quad (5)$$

After obtaining the depth predictions, the depth values are unprojected as the center of the 3DGS. The cost volume and image feature are then decoded to obtain other Gaussian parameters, similar to MVSpLat [8].

Incremental Fusion. To reduce the redundancy of Gaussians, we achieve the incremental fusion by updating G_{local}^i to G_{global}^{i+1} using a depth constraint. Specifically, given G_{local}^i with a 2D coordinate $[x_{local}, y_{local}]$ and depth d_{local} , we project all global Gaussians $\{\mu_{global}^j\}_{j=1}^K$ from G_{global}^i onto the current pixel coordinate system using the camera projection matrix \mathbf{P}^i :

$$[x_j^g, y_j^g, d_j^g]^\top = \mathbf{P}^i \mu_{global}^j, \quad (6)$$

We then construct a candidate set of global Gaussians projected to the same discrete pixel location via:

$$\mathcal{S}_{global} = \{j \mid [x_j^g] = x_{local} \wedge [y_j^g] = y_{local}\}. \quad (7)$$

To enforce geometric continuity, we prune conflicting Gaussians from \mathcal{S}_{global} that violate the depth consistency constraint. The Gaussians to be pruned are those in \mathcal{C} , defined as:

$$\mathcal{C} = \{j \in \mathcal{S}_{global} \mid |d_{local} - d_j^g| < \delta \cdot d_{local}\}, \quad (8)$$

where δ controls the depth tolerance. The global model is then updated by selectively merging the valid local Gaussians, which are those not included in \mathcal{C} , into the existing global model, as shown by:

$$G_{global}^{i+1} \leftarrow G_{global}^i \cup (G_{local}^i \setminus \mathcal{C}). \quad (9)$$

Training of StepSplat. Traditional 3DGS feed-forward methods [7, 8, 28, 52] struggle to meet the demands of interactive 3D scene generation. This is partly due to the limited diversity of datasets, which focus on specific scenes such as autonomous driving [6, 44] or indoor environments [12, 43]. Additionally, there is a significant gap between the viewpoint variations in these datasets and the requirements of interactive 3D scene generation. To address this challenge, we create a dataset utilizing 3D generation models [10, 21, 34, 64, 65] with simulated viewpoint changes for the purpose of training StepSplat, which is detailed in Section 3.5. During training, we randomly select an image sequence and feed these images into the model one by one to generate a global Gaussian representation. This representation is then used to render images from novel viewpoints, with the RGB images serving as supervision.

3.3. QuickDepth

In the field of depth completion, existing methods [18, 27–29, 58] have made notable advancements. However, these

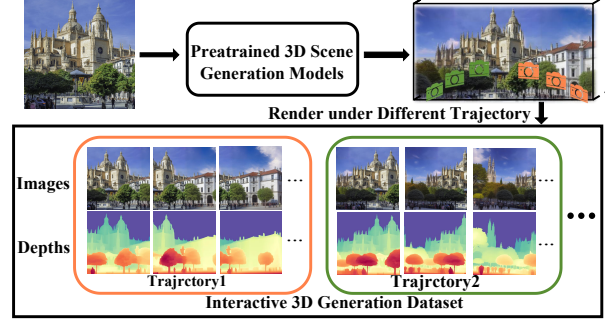


Figure 4. The process of constructing the interactive 3D generation dataset.

methods are generally designed for sparse depth completion and face challenges in completing depth for regions that lack any depth information, a critical requirement for interactive 3D scene generation. To address this, WonderWorld [64] introduces a training-free guided depth diffusion method, but it requires over 3 seconds per depth map. Invisible Stitch [14] trains a depth completion model through teacher distillation and self-training due to the lack of ground-truth data. However, its training data are limited, leading to a decline in performance in some scenarios. We introduce *QuickDepth*, a lightweight depth completion model trained on our constructed dataset for interactive 3D scene generation, with strong generalization capabilities, performing well across a wide range of scenarios.

To adapt *QuickDepth* to interactive 3D scene generation, we construct a dataset comprising diverse scenes, including indoor and outdoor environments, and scenes from comics and artworks (detailed in Section 3.5). Instead of using random masks or projections to simulate the mask in interactive 3D scene generation [14], we design a series of camera trajectories that are more aligned with interactive 3D scene generation. Specifically, we design camera poses $\{T_1, \dots, T_n\}$ and obtain frames $\{I_1, \dots, I_n\}$ along with their corresponding depth maps $\{D_1, \dots, D_n\}$ from the dataset. We then utilize the geometric relationships between adjacent frames. More precisely, for each frame I_j ($j \in [1, n]$), we project the depth map of the previous frame D_{j-1} into the coordinate system of I_j using the relative pose $T_{j-1 \rightarrow j}$. This process produces incomplete depth $D'_{j-1 \rightarrow j}$ and binary validity mask $M_{j-1 \rightarrow j}$, where invalid pixels indicate regions that require depth completion.

During training, we construct inputs by either masking the target frame’s ground truth depth D_j entirely or selecting a warped depth-mask pair $(D'_{j-1 \rightarrow j}, M_{j-1 \rightarrow j})$. Meanwhile, *QuickDepth* is initialized with a light pre-trained depth estimation model [3] and takes as input the target frame’s RGB image, the incomplete depth map and the binary mask. It then predicts the full depth, where the prediction is supervised by the target’s ground truth depth through a L_1 loss.

3.4. FastPaint

In 3D scene generation, image inpainting [31, 48, 63, 67] is crucial for modeling 3D appearance. Some methods, like Pano2Room [34], generate panoramic images from a single input but struggle to place content at user-specified locations. Others, such as WonderJourney [65] and WonderWorld [64], use Stable Diffusion-based fine-tuned inpainting models [37]. However, during fine-tuning, the inpainting regions differ significantly from those in 3D scene generation, requiring a separate model to verify generated content for each instance [65]. Moreover, these diffusion models need multiple inference steps. To address this, we propose *FastPaint*, which reduces inference to 2 steps and enhances pretrained models’ inpainting capability through distillation and fine-tuning, making them suitable for interactive 3D generation.

Specifically, our approach synergistically leverages the advantages of ODE trajectory preservation and reformulation [36] to perform knowledge distillation [19] on the pretrained model [37], reducing the number of inference steps required while maintaining the quality of appearance modeling. To address the issue where inpainting regions in 3D scene generation differ from those in fine-tuning, a dataset is constructed for training *FastPaint*. Especially, we designed camera poses to simulate the interactive 3D generation process. By obtaining depth maps and images and using projections to acquire masks, we ensure the dataset aligns with the specific requirements of the inpainting task in this context. The construction of this dataset shares similarities with the methodology used in *StepSplat* and *QuickDepth*, particularly in simulating camera trajectories to help the models adapt to interactive 3D scene generation.

3.5. Interactive 3D Generation Dataset

Interactive 3D generation from a single image allows for a wide variety of images with different styles to be used as inputs. However, real-world data is often limited to a few specific scenes, mainly in autonomous driving [6, 44] or indoor environments [12, 43]. This limitation results in poor generalization for current 3D generation methods [10, 34, 71]. Meanwhile, some methods [64, 65] directly use pretrained models to construct the pipeline, which may not be tailored for 3D interactive scene generation, resulting in the need for a Vision-Language Model (VLM) [1, 24, 70] to verify if the generated content matches the scene style or textual requirements.

To overcome this limitation, we build a dataset based on current 3D scene generation methods and train all our modules using this dataset. Specifically, we employ multiple 3D scene generation methods [10, 21, 34, 41, 64, 65, 68, 71] to create 3D scenes that each method excels at. Meanwhile, a VLM model [65] is used to verify whether the generated data conforms to the defined scene. Finally, the

dataset contains over 6 million frames rendered through simulated interactive trajectories, including rotational paths, linear movements, and hybrid trajectories. The dataset primarily covers four categories: indoor environments (32%), urban landscapes (28%), natural terrains (25%), and stylized artistic scenes (15%). When training *StepSplat*, we impose certain restrictions on the distances between adjacent frames as inputs for *StepSplat*. This is to avoid using frames that are too close together, ensuring better alignment with the practical application of 3D interactive generation. For *FastPaint* and *QuickDepth*, the depth of two adjacent frames is used to project and obtain the corresponding mask.

4. Experiments

In this section, we present our experimental setup, which includes implementation details and evaluation metrics. Subsequently, both quantitative and qualitative results are provided to demonstrate the superiority of *WonderTurbo* in performance and efficiency. Finally, we conduct ablation studies to validate the effectiveness of each module.

4.1. Experiment Setup

Baselines. In our comparative analysis, we select representative 3D generation methods, encompassing both offline and online approaches [10, 21, 34, 64, 65, 71]. The offline methods include LucidDreamer [10] and Text2Room [21], which generate 3D scenes by producing multi-view images of a scene, as well as Pano2Room [34] and DreamScene360 [71], which directly generate panoramic images that are then elevated to 3D. For online 3D scene generation, we evaluate WonderJourney [65] and WonderWorld [64]. All comparisons are conducted using the official codebases provided by these methods.

Evaluation Metrics. To evaluate the quality of 3D scene generation, following WonderWorld [64], we used CLIP [35] scores (CS), CLIP [35] consistency (CC), CLIP-IQA+ [49] (CIQA), Q-Align [53], and CLIP aesthetic [35] scores (CA) as metrics. Additionally, a user study is conducted to gather subjective feedback on visual quality. More details are provided in the supplementary materials.

Implementation Details. To ensure comprehensive evaluation, we use input images from LucidDreamer [10], WonderJourney [65], and WonderWorld [64]. We generate 8 scenes for each of 4 test cases, totaling 32 scenes. Evaluations are conducted with a fixed panoramic camera. For efficiency, we compare the time taken to generate scenes of the same size within the camera’s view. More details are in the supplementary materials.

4.2. Main Results

Generation Speed. The time cost is crucial for interactive 3D scene generation. However, despite utilizing FLAGS for acceleration, WonderWorld [64], the fastest among the



Prompt: Roads, Temples, Cathedrals, Snow mountains Prompt: Gardens, Trees, Offices, Cafe

Figure 5. Qualitative comparisons of using a fixed panoramic camera path.

compared methods, still requires more than 10 seconds to generate a scene as shown in Tab. 1. LucidDreamer [10] and Text2Room [21] involve generating multiple views for each new scene, substantially increasing the time devoted to modeling appearance. While Pano2Room [34] and DreamScene360 [71] do not generate multiple perspectives, the inherent delays in panoramic image generation and the neces-

sity for per-scene optimization significantly constrain their efficiency. Notably, *WonderTurbo* excels in both geometry and appearance modeling, accelerating overall time by 15 \times .

Quantitative Results. In Tab. 2, we compare *WonderTurbo* with various 3D scene generation methods [10, 21, 34, 64, 65, 71]. The experimental results show that online 3D scene generation methods outperform offline approaches by better

Table 1. Time comparison of scene generation, including geometry and appearance modeling, on an H20 GPU for offline and online methods. We compare the time taken to generate scenes of the same size within the camera’s view.

	Method	Geometry (s)	Appearance (s)	Total (s)
Offline	LucidDreamer [10]	35.38	8.32	43.70
	Text2Room [21]	34.23	7.32	41.55
	Pano2Room [34]	27.91	1.47	29.38
	DreamScene360 [71]	44.29	1.45	45.74
Online	WonderJourney [65]	78.12	1.45	79.57
	WonderWorld [64]	6.62	4.43	11.05
	<i>WonderTurbo</i>	0.50	0.22	0.72

Table 2. Evaluation of novel view renderings for offline and online methods

	Method	CS \uparrow	CC \uparrow	CIQA \uparrow	Q-Align \uparrow	CA \uparrow
Offline	LucidDreamer [10]	27.72	0.9213	0.6023	3.5439	6.8231
	Text2Room [21]	24.50	0.9035	0.4910	2.6732	6.5324
	Pano2Room [34]	25.67	0.8652	0.3534	2.1342	5.0367
	DreamScene360 [71]	24.50	0.8435	4.6973	2.4620	6.9846
Online	WonderJourney [65]	27.63	0.9652	0.4753	3.5276	7.0134
	WonderWorld [64]	28.14	0.9654	0.6764	3.7823	7.2121
	<i>WonderTurbo</i>	28.65	0.9732	0.6812	3.7253	7.3243

Table 3. Comparing the win rates of *WonderTurbo* in rendering novel views.

	Method	Win Rate	Method	Win Rate
	vs. LucidDreamer [10]	96.32%	vs. Text2Room [21]	98.47%
	vs. Pano2Room [34]	94.26%	vs. DreamScene360 [71]	96.23%
	vs. WonderJourney [65]	96.54%	vs. WonderWorld [64]	69.43%

meeting user textual requirements, achieving higher CLIP scores and improved CLIP consistency. WonderWorld [64] surpasses all other baseline methods, leading across all metrics. However, even with a $15\times$ acceleration, *WonderTurbo* maintains competitive performance across all metrics compared to WonderWorld [64]. Additionally, since *WonderTurbo* is fine-tuned specifically for interactive 3D generation tasks, improvements are observed in CLIP scores, CLIP consistency, CLIP-IQA+ and CLIP aesthetic.

User Study. Additionally, we conduct a user study to evaluate the quality of 3D scenes generated by various methods. As shown in Tab. 3, the results indicate that *WonderTurbo* achieves comparable performance to WonderWorld [64] with a lower scene generation time cost and significantly outperforms all other methods in terms of user preference.

Qualitative Results. As shown in Fig. 5, we present a qualitative comparison between *WonderTurbo* and several baseline methods using the same settings. Notably, *WonderTurbo* delivers competitive scene generation quality while significantly reducing generation time. In contrast, DreamScene360 [71] and Pano2Room [34] struggle with noticeable geometric distortions and lack aesthetic appeal due to limited generalization capabilities. Meanwhile, LucidDreamer [10] and Text2Room [21] fail to place content correctly, with some prompt details not materializing. The re-

Table 4. Ablation study results on different geometry models.

	CS \uparrow	CC \uparrow	CIQA \uparrow	Q-Align \uparrow	CA \uparrow
<i>WonderTurbo</i> w/ FreeSplat	27.65	0.9542	0.6460	3.1543	6.6235
<i>WonderTurbo</i> w/ DepthSplat	27.32	0.9675	0.6620	3.2145	6.7432
<i>WonderTurbo</i> w/ <i>StepSplat</i>	28.65	0.9732	0.6812	3.7253	7.3243

Table 5. Ablation study results on novel view renderings.

	CS \uparrow	CC \uparrow	CIQA \uparrow	Q-Align \uparrow	CA \uparrow
Ours w/o depth guided	27.72	0.9532	0.6359	3.4361	7.1734
Ours w/o incremental fusion	27.87	0.9654	0.6459	3.5431	7.2734
Ours w/o <i>FastPaint</i>	27.82	0.9683	0.6574	3.7146	7.2136
<i>WonderTurbo</i>	28.65	0.9732	0.6812	3.7253	7.3243

sults from *WonderTurbo* and WonderWorld [64] are closely matched, both demonstrating strong performance.

4.3. Ablation Study

Geometry Modeling. We compare different geometry modeling methods, including FreeSplat [52] and DepthSplat [54], all fine-tuned with the same settings for fairness. As shown in Tab. 4, FreeSplat [52] and DepthSplat [28] underperform compared to *StepSplat*, especially in Q-Align and CLIP aesthetic scores, due to their reliance on unsupervised depth estimation. In contrast, *StepSplat* uses a consistent depth map to guide cost volume construction, enabling adaptive interactive 3D scene generation.

StepSplat. We conduct ablation experiments on *StepSplat* to illustrate the effect of the depth guided cost volume and the incremental infusion. As shown in Tab. 5, the depth-guided cost volume is key to accurate geometry modeling and image quality. Meanwhile, incremental fusion improves performance by reducing redundant Gaussians and avoiding floating-point issues.

FastPaint. We compare *FastPaint* with the pretrained inpainting model [37]. As shown in Tab. 5, *FastPaint* enhances the capability of 3D appearance modeling, with improvements across various metrics.

5. Discussion and Conclusion

Despite progress in 3D scene generation from a single image, efficiency remains a challenge due to time-consuming geometry optimization and viewpoint refinement. To address this, we propose *WonderTurbo*, an efficient framework for real-time interactive 3D scene generation that accelerates geometry optimization and appearance modeling. For accelerating geometry modeling, we introduce *StepSplat*, which expands 3D scenes within 0.26 seconds while maintaining high visual quality, and *QuickDepth*, which provides consistent depth priors for cost volume construction. For appearance modeling, *FastPaint* is proposed to accomplish appearance modeling with only 2 inference steps while ensuring spatial consistency. Experiments show that *WonderTurbo* accurately generates 3D scenes from text, outperforming CLIP-based metrics and user study win rates, with a $15\times$ speedup.

References

- [1] Shuai Bai, Keqin Chen, Xuejing Liu, Jialin Wang, Wenbin Ge, Sibao Song, Kai Dang, Peng Wang, Shijie Wang, Jun Tang, et al. Qwen2. 5-vl technical report. *arXiv preprint arXiv:2502.13923*, 2025. 3, 6
- [2] Miguel Angel Bautista, Pengsheng Guo, Samira Abnar, Walter Talbott, Alexander Toshev, Zhuoyuan Chen, Laurent Dinh, Shuangfei Zhai, Hanlin Goh, Daniel Ulbricht, et al. Gaudi: A neural architect for immersive 3d scene generation. *Advances in Neural Information Processing Systems*, 35:25102–25116, 2022. 2
- [3] Shariq Farooq Bhat, Reiner Birkl, Diana Wofk, Peter Wonka, and Matthias Müller. Zoedepth: Zero-shot transfer by combining relative and metric depth. *arXiv preprint arXiv:2302.12288*, 2023. 5
- [4] Xiao Bi, Deli Chen, Guanting Chen, Shanhuang Chen, Damai Dai, Chengqi Deng, Honghui Ding, Kai Dong, Qiusi Du, Zhe Fu, et al. Deepseek llm: Scaling open-source language models with longtermism. *arXiv preprint arXiv:2401.02954*, 2024. 3
- [5] Tom Brown, Benjamin Mann, Nick Ryder, Melanie Subbiah, Jared D Kaplan, Prafulla Dhariwal, Arvind Neelakantan, Pranav Shyam, Girish Sastry, Amanda Askell, et al. Language models are few-shot learners. *Advances in neural information processing systems*, 33:1877–1901, 2020. 3
- [6] Holger Caesar, Varun Bankiti, Alex H Lang, Sourabh Vora, Venice Erin Liang, Qiang Xu, Anush Krishnan, Yu Pan, Giancarlo Baldan, and Oscar Beijbom. nuscenes: A multi-modal dataset for autonomous driving. In *CVPR*, 2020. 5, 6
- [7] David Charatan, Sizhe Lester Li, Andrea Tagliasacchi, and Vincent Sitzmann. pixelsplat: 3d gaussian splats from image pairs for scalable generalizable 3d reconstruction. In *Proceedings of the IEEE/CVF conference on computer vision and pattern recognition*, pages 19457–19467, 2024. 2, 3, 5
- [8] Yuedong Chen, Haofei Xu, Chuanxia Zheng, Bohan Zhuang, Marc Pollefeys, Andreas Geiger, Tat-Jen Cham, and Jianfei Cai. Mvsplat: Efficient 3d gaussian splatting from sparse multi-view images. In *European Conference on Computer Vision*, pages 370–386. Springer, 2024. 2, 3, 5
- [9] Yuedong Chen, Chuanxia Zheng, Haofei Xu, Bohan Zhuang, Andrea Vedaldi, Tat-Jen Cham, and Jianfei Cai. Mvsplat360: Feed-forward 360 scene synthesis from sparse views. *Advances in Neural Information Processing Systems*, 37:107064–107086, 2025. 3
- [10] Jaeyoung Chung, Suyoung Lee, Hyeongjin Nam, Jaerin Lee, and Kyoung Mu Lee. Luciddreamer: Domain-free generation of 3d gaussian splatting scenes. *arXiv preprint arXiv:2311.13384*, 2023. 2, 5, 6, 7, 8, 12
- [11] Robert T Collins. A space-sweep approach to true multi-image matching. In *Proceedings CVPR IEEE computer society conference on computer vision and pattern recognition*, pages 358–363. Ieee, 1996. 4
- [12] Angela Dai, Angel X Chang, Manolis Savva, Maciej Halber, Thomas Funkhouser, and Matthias Nießner. Scannet: Richly-annotated 3d reconstructions of indoor scenes. In *Proceedings of the IEEE conference on computer vision and pattern recognition*, pages 5828–5839, 2017. 5, 6
- [13] Xiaohan Ding, Xiangyu Zhang, Ningning Ma, Jungong Han, Guiguang Ding, and Jian Sun. Repvgg: Making vgg-style convnets great again. In *Proceedings of the IEEE/CVF conference on computer vision and pattern recognition*, pages 13733–13742, 2021. 4
- [14] Paul Engstler, Andrea Vedaldi, Iro Laina, and Christian Rupprecht. Invisible stitch: Generating smooth 3d scenes with depth inpainting. *arXiv preprint arXiv:2404.19758*, 2024. 5
- [15] Dave Epstein, Ben Poole, Ben Mildenhall, Alexei A Efros, and Aleksander Holynski. Disentangled 3d scene generation with layout learning. *arXiv preprint arXiv:2402.16936*, 2024. 2
- [16] Mengyang Feng, Jinlin Liu, Miaomiao Cui, and Xuansong Xie. Diffusion360: Seamless 360 degree panoramic image generation based on diffusion models. *arXiv preprint arXiv:2311.13141*, 2023. 3, 12
- [17] Ziyue Feng, Liang Yang, Longlong Jing, Haiyan Wang, YingLi Tian, and Bing Li. Disentangling object motion and occlusion for unsupervised multi-frame monocular depth. In *European Conference on Computer Vision*, pages 228–244. Springer, 2022. 4
- [18] Eric Ghysels, Arthur Sinko, and Rossen Valkanov. Midas regressions: Further results and new directions. *Econometric reviews*, 26(1):53–90, 2007. 5
- [19] Jianping Gou, Baosheng Yu, Stephen J Maybank, and Dacheng Tao. Knowledge distillation: A survey. *International Journal of Computer Vision*, 129(6):1789–1819, 2021. 6
- [20] Daya Guo, Qihao Zhu, Dejian Yang, Zhenda Xie, Kai Dong, Wentao Zhang, Guanting Chen, Xiao Bi, Yu Wu, YK Li, et al. Deepseek-coder: When the large language model meets programming—the rise of code intelligence. *arXiv preprint arXiv:2401.14196*, 2024. 3
- [21] Lukas Höllein, Ang Cao, Andrew Owens, Justin Johnson, and Matthias Nießner. Text2room: Extracting textured 3d meshes from 2d text-to-image models. In *Proceedings of the IEEE/CVF International Conference on Computer Vision*, pages 7909–7920, 2023. 2, 5, 6, 7, 8, 12
- [22] Binbin Huang, Zehao Yu, Anpei Chen, Andreas Geiger, and Shenghua Gao. 2d gaussian splatting for geometrically accurate radiance fields. In *ACM SIGGRAPH 2024 conference papers*, pages 1–11, 2024. 3
- [23] Bernhard Kerbl, Georgios Kopanas, Thomas Leimkühler, and George Drettakis. 3d gaussian splatting for real-time radiance field rendering. *ACM Trans. Graph.*, 42(4):139–1, 2023. 2, 3
- [24] Weicheng Kuo, Yin Cui, Xiuye Gu, AJ Piergiovanni, and Anelia Angelova. F-vlm: Open-vocabulary object detection upon frozen vision and language models. *arXiv preprint arXiv:2209.15639*, 2022. 3, 6
- [25] Haoran Li, Haolin Shi, Wenli Zhang, Wenjun Wu, Yong Liao, Lin Wang, Lik-hang Lee, and Peng Yuan Zhou. Dreamscene: 3d gaussian-based text-to-3d scene generation via formation pattern sampling. In *European Conference on Computer Vision*, pages 214–230. Springer, 2024. 2

- [26] Hanwen Liang, Junli Cao, Vidit Goel, Guocheng Qian, Sergei Korolev, Demetri Terzopoulos, Konstantinos N. Plataniotis, Sergey Tulyakov, and Jian Ren. Wonderland: Navigating 3d scenes from a single image, 2024. [2](#)
- [27] Lina Liu, Xibin Song, Xiaoyang Lyu, Junwei Diao, Mengmeng Wang, Yong Liu, and Liangjun Zhang. Fcfr-net: Feature fusion based coarse-to-fine residual learning for depth completion. In *Proceedings of the AAAI conference on artificial intelligence*, pages 2136–2144, 2021. [5](#)
- [28] Zhiheng Liu, Ka Leong Cheng, Qiuyu Wang, Shuzhe Wang, Hao Ouyang, Bin Tan, Kai Zhu, Yujun Shen, Qifeng Chen, and Ping Luo. Depthlab: From partial to complete. *arXiv preprint arXiv:2412.18153*, 2024. [5](#), [8](#)
- [29] Zhiheng Liu, Hao Ouyang, Qiuyu Wang, Ka Leong Cheng, Jie Xiao, Kai Zhu, Nan Xue, Yu Liu, Yujun Shen, and Yang Cao. Infusion: Inpainting 3d gaussians via learning depth completion from diffusion prior. *arXiv preprint arXiv:2404.11613*, 2024. [5](#)
- [30] Taiming Lu, Tianmin Shu, Junfei Xiao, Luoxin Ye, Jiahao Wang, Cheng Peng, Chen Wei, Daniel Khashabi, Rama Chellappa, Alan Yuille, et al. Genex: Generating an explorable world. *arXiv preprint arXiv:2412.09624*, 2024. [2](#), [3](#)
- [31] Zhuqiang Lu, Kun Hu, Chaoyue Wang, Lei Bai, and Zhiyong Wang. Autoregressive omni-aware outpainting for open-vocabulary 360-degree image generation. In *Proceedings of the AAAI Conference on Artificial Intelligence*, pages 14211–14219, 2024. [6](#)
- [32] Chaojun Ni, Guosheng Zhao, Xiaofeng Wang, Zheng Zhu, Wenkang Qin, Guan Huang, Chen Liu, Yuyin Chen, Yida Wang, Xueyang Zhang, et al. Recondreamer: Crafting world models for driving scene reconstruction via online restoration. *arXiv preprint arXiv:2411.19548*, 2024. [2](#), [3](#)
- [33] Simon Niklaus, Long Mai, Jimei Yang, and Feng Liu. 3d ken burns effect from a single image. *ACM Transactions on Graphics (ToG)*, 38(6):1–15, 2019. [2](#)
- [34] Guo Pu, Yiming Zhao, and Zhouhui Lian. Pano2room: Novel view synthesis from a single indoor panorama. In *SIGGRAPH Asia 2024 Conference Papers*, pages 1–11, 2024. [2](#), [3](#), [5](#), [6](#), [7](#), [8](#)
- [35] Alec Radford, Jong Wook Kim, Chris Hallacy, Aditya Ramesh, Gabriel Goh, Sandhini Agarwal, Girish Sastry, Amanda Askell, Pamela Mishkin, Jack Clark, et al. Learning transferable visual models from natural language supervision. In *ICML*, 2021. [2](#), [6](#), [12](#)
- [36] Yuxi Ren, Xin Xia, Yanzuo Lu, Jiacheng Zhang, Jie Wu, Pan Xie, Xing Wang, and Xuefeng Xiao. Hyper-sd: Trajectory segmented consistency model for efficient image synthesis. *Advances in Neural Information Processing Systems*, 37:117340–117362, 2025. [6](#)
- [37] Robin Rombach, Andreas Blattmann, Dominik Lorenz, Patrick Esser, and Björn Ommer. High-resolution image synthesis with latent diffusion models. In *Proceedings of the IEEE/CVF conference on computer vision and pattern recognition*, pages 10684–10695, 2022. [2](#), [3](#), [6](#), [8](#)
- [38] Olaf Ronneberger, Philipp Fischer, and Thomas Brox. U-net: Convolutional networks for biomedical image segmentation. In *Medical image computing and computer-assisted intervention—MICCAI 2015: 18th international conference, Munich, Germany, October 5–9, 2015, proceedings, part III 18*, pages 234–241. Springer, 2015. [4](#)
- [39] Shuwei Shao, Zhongcai Pei, Weihai Chen, Xingming Wu, Zhong Liu, and Zhengguo Li. Smudlp: Self-teaching multi-frame unsupervised endoscopic depth estimation with learnable patchmatch. *arXiv preprint arXiv:2205.15034*, 2022. [4](#)
- [40] Meng-Li Shih, Shih-Yang Su, Johannes Kopf, and Jia-Bin Huang. 3d photography using context-aware layered depth inpainting. In *Proceedings of the IEEE/CVF Conference on Computer Vision and Pattern Recognition*, pages 8028–8038, 2020. [2](#)
- [41] Jaidev Shriram, Alex Trevithick, Lingjie Liu, and Ravi Ramamoorthi. Realdreamer: Text-driven 3d scene generation with inpainting and depth diffusion. *arXiv preprint arXiv:2404.07199*, 2024. [6](#)
- [42] Brandon Smart, Chuanxia Zheng, Iro Laina, and Victor Adrian Prisacariu. Splatt3r: Zero-shot gaussian splatting from uncalibrated image pairs. *arXiv preprint arXiv:2408.13912*, 2024. [3](#)
- [43] Julian Straub, Thomas Whelan, Lingni Ma, Yufan Chen, Erik Wijmans, Simon Green, Jakob J Engel, Raul Mur-Artal, Carl Ren, Shobhit Verma, et al. The replica dataset: A digital replica of indoor spaces. *arXiv preprint arXiv:1906.05797*, 2019. [5](#), [6](#)
- [44] Pei Sun, Henrik Kretzschmar, Xerxes Dotiwalla, Aurelien Chouard, Vijaysai Patnaik, Paul Tsui, James Guo, Yin Zhou, Yuning Chai, Benjamin Caine, Vijay Vasudevan, Wei Han, Jiquan Ngiam, Hang Zhao, Aleksei Timofeev, Scott Etinger, Maxim Krivokon, Amy Gao, Aditya Joshi, Yu Zhang, Jonathon Shlens, Zhifeng Chen, and Dragomir Anguelov. Scalability in perception for autonomous driving: Waymo open dataset. In *CVPR*, 2020. [5](#), [6](#)
- [45] Richard Tucker and Noah Snavely. Single-view view synthesis with multiplane images. In *Proceedings of the IEEE/CVF Conference on Computer Vision and Pattern Recognition*, pages 551–560, 2020. [2](#)
- [46] Shubham Tulsiani, Richard Tucker, and Noah Snavely. Layer-structured 3d scene inference via view synthesis. In *Proceedings of the European Conference on Computer Vision (ECCV)*, pages 302–317, 2018.
- [47] Boyuan Wang, Xiaofeng Wang, Chaojun Ni, Guosheng Zhao, Zhiqin Yang, Zheng Zhu, MUYANG Zhang, Yukun Zhou, Xinze Chen, Guan Huang, Lihong Liu, and Xingang Wang. Humandreamer: Generating controllable human-motion videos via decoupled generation. *arXiv preprint arXiv:2503.24026*, 2025. [2](#)
- [48] Fu-Yun Wang, Xiaoshi Wu, Zhaoyang Huang, Xiaoyu Shi, Dazhong Shen, Guanglu Song, Yu Liu, and Hongsheng Li. Be-your-outpainter: Mastering video outpainting through input-specific adaptation. In *European Conference on Computer Vision*, pages 153–168. Springer, 2024. [6](#)
- [49] Jianyi Wang, Kelvin CK Chan, and Chen Change Loy. Exploring clip for assessing the look and feel of images. In *Proceedings of the AAAI conference on artificial intelligence*, pages 2555–2563, 2023. [2](#), [6](#), [12](#)
- [50] Xiaofeng Wang, Zheng Zhu, Guan Huang, Xinze Chen, Jiakang Zhu, and Jiwen Lu. Drivedreamer: Towards real-world-

- driven world models for autonomous driving. *arXiv preprint arXiv:2309.09777*, 2023. 3
- [51] Xiaofeng Wang, Zheng Zhu, Guan Huang, Xu Chi, Yun Ye, Ziwei Chen, and Xingang Wang. Crafting monocular cues and velocity guidance for self-supervised multi-frame depth learning. In *Proceedings of the AAAI Conference on Artificial Intelligence*, pages 2689–2697, 2023. 3, 4
- [52] Yunsong Wang, Tianxin Huang, Hanlin Chen, and Gim Hee Lee. Freesplat: Generalizable 3d gaussian splatting towards free view synthesis of indoor scenes. *Advances in Neural Information Processing Systems*, 37:107326–107349, 2025. 2, 3, 5, 8
- [53] Haoning Wu, Zicheng Zhang, Weixia Zhang, Chaofeng Chen, Liang Liao, Chunyi Li, Yixuan Gao, Annan Wang, Erli Zhang, Wenxiu Sun, et al. Q-align: Teaching Imms for visual scoring via discrete text-defined levels. *arXiv preprint arXiv:2312.17090*, 2023. 6, 12
- [54] Haofei Xu, Songyou Peng, Fangjinhua Wang, Hermann Blum, Daniel Barath, Andreas Geiger, and Marc Pollefeys. Depthsplat: Connecting gaussian splatting and depth. *arXiv preprint arXiv:2410.13862*, 2024. 2, 3, 8
- [55] Yunzhi Yan, Haotong Lin, Chenxu Zhou, Weijie Wang, Haiyang Sun, Kun Zhan, Xianpeng Lang, Xiaowei Zhou, and Sida Peng. Street gaussians: Modeling dynamic urban scenes with gaussian splatting. In *European Conference on Computer Vision*, pages 156–173. Springer, 2024. 2
- [56] Yunzhi Yan, Haotong Lin, Chenxu Zhou, Weijie Wang, Haiyang Sun, Kun Zhan, Xianpeng Lang, Xiaowei Zhou, and Sida Peng. Street gaussians for modeling dynamic urban scenes. *arXiv preprint arXiv:2401.01339*, 2024. 3
- [57] An Yang, Baosong Yang, Beichen Zhang, Binyuan Hui, Bo Zheng, Bowen Yu, Chengyuan Li, Dayiheng Liu, Fei Huang, Haoran Wei, et al. Qwen2. 5 technical report. *arXiv preprint arXiv:2412.15115*, 2024. 3
- [58] Lihe Yang, Bingyi Kang, Zilong Huang, Xiaogang Xu, Jiashi Feng, and Hengshuang Zhao. Depth anything: Unleashing the power of large-scale unlabeled data. In *Proceedings of the IEEE/CVF Conference on Computer Vision and Pattern Recognition*, pages 10371–10381, 2024. 3, 5
- [59] Xiuyu Yang, Yunze Man, Junkun Chen, and Yu-Xiong Wang. Scenecraft: Layout-guided 3d scene generation. *Advances in Neural Information Processing Systems*, 37: 82060–82084, 2025. 2
- [60] Ziyi Yang, Xinyu Gao, Wen Zhou, Shaohui Jiao, Yuqing Zhang, and Xiaogang Jin. Deformable 3d gaussians for high-fidelity monocular dynamic scene reconstruction. In *Proceedings of the IEEE/CVF conference on computer vision and pattern recognition*, pages 20331–20341, 2024. 2, 3
- [61] Botao Ye, Sifei Liu, Haofei Xu, Xueting Li, Marc Pollefeys, Ming-Hsuan Yang, and Songyou Peng. No pose, no problem: Surprisingly simple 3d gaussian splats from sparse unposed images. *arXiv preprint arXiv:2410.24207*, 2024. 3
- [62] Weicai Ye, Chenhao Ji, Zheng Chen, Junyao Gao, Xiaoshui Huang, Song-Hai Zhang, Wanli Ouyang, Tong He, Cairong Zhao, and Guofeng Zhang. Diffpano: Scalable and consistent text to panorama generation with spherical epipolar-aware diffusion. *Advances in Neural Information Processing Systems*, 37:1304–1332, 2025. 3
- [63] Hang Yu, Ruilin Li, Shaorong Xie, and Jiayan Qiu. Shadow-enlightened image outpainting. In *Proceedings of the IEEE/CVF Conference on Computer Vision and Pattern Recognition*, pages 7850–7860, 2024. 6
- [64] Hong-Xing Yu, Haoyi Duan, Charles Herrmann, William T Freeman, and Jiajun Wu. Wonderworld: Interactive 3d scene generation from a single image. *arXiv preprint arXiv:2406.09394*, 2024. 2, 3, 5, 6, 7, 8
- [65] Hong-Xing Yu, Haoyi Duan, Junhwa Hur, Kyle Sargent, Michael Rubinstein, William T Freeman, Forrester Cole, Deqing Sun, Noah Snaveley, Jiajun Wu, et al. Wonderjourney: Going from anywhere to everywhere. In *Proceedings of the IEEE/CVF Conference on Computer Vision and Pattern Recognition*, pages 6658–6667, 2024. 2, 3, 5, 6, 7, 8
- [66] Jingbo Zhang, Xiaoyu Li, Ziyu Wan, Can Wang, and Jing Liao. Text2nerf: Text-driven 3d scene generation with neural radiance fields. *IEEE Transactions on Visualization and Computer Graphics*, 30(12):7749–7762, 2024. 2
- [67] Shaofeng Zhang, Jinfa Huang, Qiang Zhou, Zhibin Wang, Fan Wang, Jiebo Luo, and Junchi Yan. Continuous-multiple image outpainting in one-step via positional query and a diffusion-based approach. *arXiv preprint arXiv:2401.15652*, 2024. 6
- [68] Songchun Zhang, Yibo Zhang, Quan Zheng, Rui Ma, Wei Hua, Hujun Bao, Weiwei Xu, and Changqing Zou. 3d-scenedreamer: Text-driven 3d-consistent scene generation. In *Proceedings of the IEEE/CVF Conference on Computer Vision and Pattern Recognition*, pages 10170–10180, 2024. 6
- [69] Guosheng Zhao, Chaojun Ni, Xiaofeng Wang, Zheng Zhu, Guan Huang, Xinze Chen, Boyuan Wang, Youyi Zhang, Wenjun Mei, and Xingang Wang. Drivedreamer4d: World models are effective data machines for 4d driving scene representation. *arXiv preprint arXiv:2410.13571*, 2024. 2
- [70] Taijin Zhao, Heqian Qiu, Yu Dai, Lanxiao Wang, Hefei Mei, Fanman Meng, Qingbo Wu, and Hongliang Li. Vlm-guided explicit-implicit complementary novel class semantic learning for few-shot object detection. *Expert Systems with Applications*, 256:124926, 2024. 6
- [71] Shijie Zhou, Zhiwen Fan, Dejia Xu, Haoran Chang, Pradyumna Chari, Tejas Bharadwaj, Suyu You, Zhangyang Wang, and Achuta Kadambi. Dreamscene360: Unconstrained text-to-3d scene generation with panoramic gaussian splatting. In *European Conference on Computer Vision*, pages 324–342. Springer, 2024. 3, 6, 7, 8, 12
- [72] Tinghui Zhou, Richard Tucker, John Flynn, Graham Fyffe, and Noah Snaveley. Stereo magnification: Learning view synthesis using multiplane images. *arXiv preprint arXiv:1805.09817*, 2018. 2

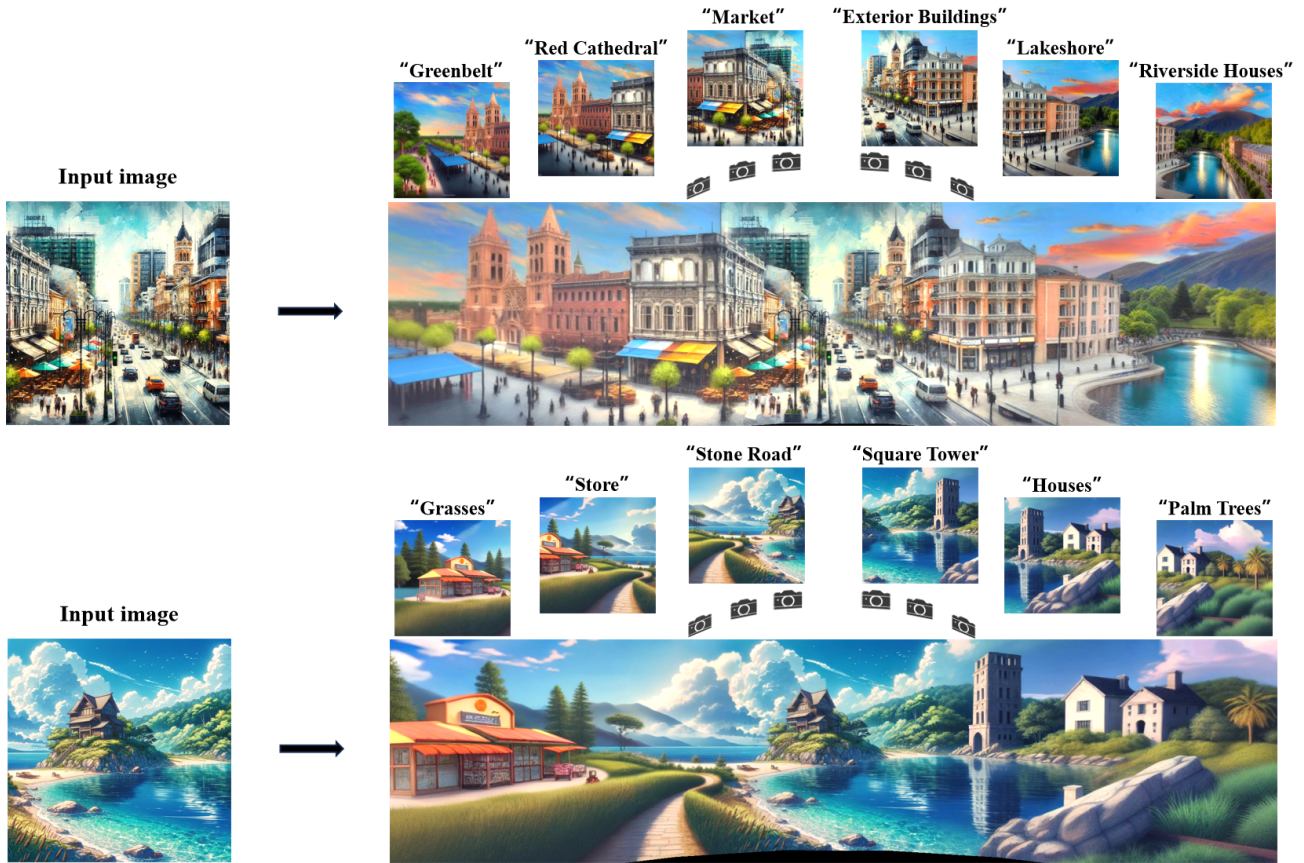


Figure 6. Qualitative examples.

1. Implementation Details

Time cost evaluation. To effectively evaluate the generated scenes, we compare the time required to generate scenes of the same size. Specifically, for offline methods, we follow the setups of LucidDreamer [10] and Text2Room [21], first generating multiple images of new scenes and then converting them into 3D scenes according to their respective methods. For DreamScene360 [71] and Text2Room [21], we use the Diffusion360 [16] model to generate panorama images of the input images, which are then lifted to 3D. We compute the total time for this process and compute the time cost of generating the test scenes based on the size of the generated and test scenes. For online methods, we directly calculate the time required to generate a new scene.

Metrics. To evaluate the quality of 3D interactive scene generation, we utilize several metrics: CLIP scores (CS) [35], CLIP consistency (CC) [35], CLIP-IQA+ (CIQA) [49], Q-Align [53], and CLIP aesthetic scores (CA) [35]. These metrics not only assess the quality of appearance modeling but also evaluate the quality of geometry modeling, as inaccurate geometry can lead to severe distortions when rendering novel views, which can significantly impact metrics such as CLIP-IQA+ (CIQA), Q-Align, and CLIP aesthetic scores (CA). The CLIP score (CS) measures the relevance between the scene prompt and the ren-

dered image by computing the cosine similarity between their respective CLIP embeddings. CLIP consistency (CC) is assessed by measuring the cosine similarity between the CLIP embeddings of each novel view and the central view, ensuring semantic consistency across views. CLIP-IQA+ (CIQA) is an enhanced image quality metric that combines perceptual quality models with deep learning techniques to evaluate attributes. Finally, the CLIP aesthetic score (CA) captures the aesthetic quality of the image, considering elements like composition, contrast, and color harmony.

2. Qualitative results

As shown in Fig. 6, Fig. 8, and Fig. 7, we provide additional scenes in various styles to demonstrate the superiority of *WonderTurbo*.



Figure 7. Qualitative examples.

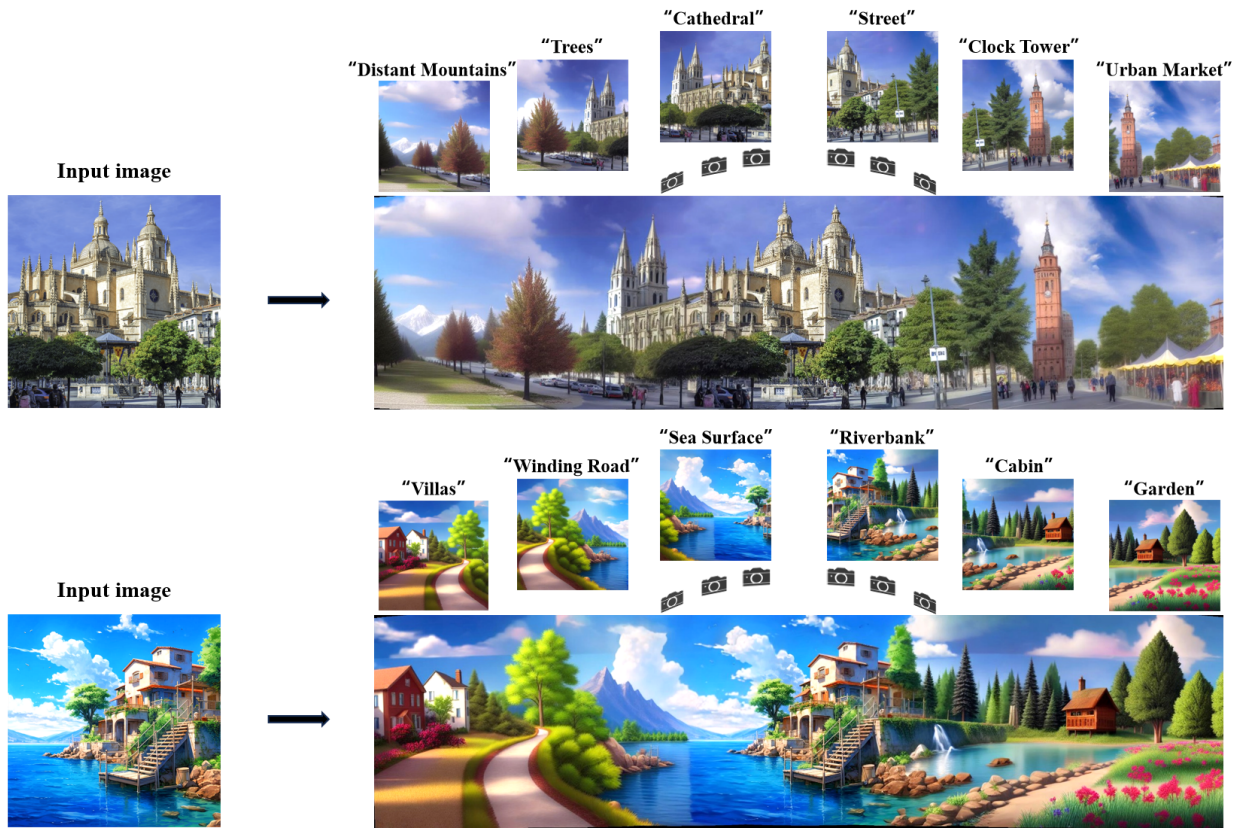


Figure 8. Qualitative examples.